Inhibition of Tau Polymerization by Its Carboxy-Terminal Caspase Cleavage Fragment†

R. W. Berry,*,‡,§ A. Abraha,‡ S. Lagalwar,‡ N. LaPointe,‡ T. C. Gamblin,‡ V. L. Cryns,|| and L. I. Binder‡,§

Department of Cell and Molecular Biology, Cognitive Neurology and Alzheimer's Disease Center, and Division of Endocrinology, Metabolism, and Molecular Medicine, Feinberg School of Medicine, Northwestern University, 303 East Chicago Avenue, Chicago, Illinois 60611

Received December 12, 2002; Revised Manuscript Received May 19, 2003

ABSTRACT: Abnormal aggregation of the microtubule-associated protein, tau, occurs in many neurodegenerative diseases, making it important to understand the mechanisms of tau polymerization. Previous work has indicated that the C-terminal region of tau inhibits polymerization in vitro, and a growing body of evidence implicates caspase cleavage of tau at Asp 421 in the C-terminus as an important inducer of tau polymerization in Alzheimer's disease. In the present study, we provide evidence that the C-terminal peptide fragment produced by caspase cleavage inhibits tau polymerization, suggesting that caspase cleavage of tau enhances its polymerization by removing the inhibitory control element. Moreover, we provide evidence that the peptide assumes an α-helical configuration and inhibits tau assembly by interacting with residues 321−375 in the microtubule binding repeat region. These findings indicate that formation of the fibrillar pathologies during the course of Alzheimer's disease may be driven or sustained by apoptotic events leading to caspase activation.

Abnormal deposits of the microtubule-associated protein tau are characteristic features of a number of neurodegenerative diseases, including Alzheimer's disease (AD),[1] Pick disease, progressive supranuclear palsy, corticobasal degeneration, and the inherited disorders collectively known as FTDP-17 (for frontotemporal dementia and Parkinsonism linked to chromosome 17) (*1*). Indeed, mutations in the tau gene are responsible for the latter, implying that abnormal tau is sufficient to cause neurodegeneration.

In the process of tau aggregation, a highly soluble molecule with little discernible secondary structure (*2*, *3*) is incorporated into a highly regular polymer. Significant structural rearrangements must accompany this transition. Since this process is a potential target for therapeutic agents, it is important to delineate its molecular details. Evidence from both in vitro and in situ studies implicates a polymerization mechanism involving truncation of tau's carboxyl-terminal region. Peptides containing little more than the microtubule binding repeat (MTBR) region are capable of polyamine-induced self-assembly in vitro (*4*), and in AD a significant proportion of neurofibrillary tangles contain tau truncated at either or both the N- and the C-termini (*5*). Moreover, recombinant tau protein truncated at various residues in the carboxy-terminal region of the molecule exhibits significantly enhanced arachidonic acid-induced polymerization in vitro, an effect that depends on the MTBR (*6*). This observation led us to postulate a model in which polymerization involves the unmasking of the microtubule binding repeat (MTBR) region, which is normally associated with the carboxy-terminal tail of the molecule (*6*).

There is accumulating evidence for a potential functional role for such truncations in AD. It has been shown that tau is a substrate for the apoptotic protease, caspase-3, in vitro and in apoptotic neurons, and that caspase-cleaved tau can be an effector of apoptosis (*7*, *8*). Exposure of cultured neurons to the amyloid Aβ peptide leads to the rapid activation of multiple caspases, including caspase-3 (*9*, *10*, and Gamblin et al., unpublished). In turn, this leads to the cleavage of tau at a highly conserved aspartate residue (Asp 421) in its C-terminus by caspase-3 and possibly other caspase family members. Finally, in AD, many neurofibrillary tangles are immunoreactive to an antibody directed against tau truncated at Asp 421 (Gamblin et al., unpublished).

While the foregoing indicates the importance of the carboxyl terminus in tau polymerization, the mechanism by which it exerts its inhibitory effect is unclear. Yet, knowledge of this mechanism could be of great importance in designing therapeutic agents for AD. We have begun to approach this problem by investigating the interactions between the peptide generated by caspase cleavage and the remainder of the tau molecule. This communication describes experiments supporting an inhibitory role for the C-terminal caspase cleavage fragment, and by extension, a stimulatory role for caspase cleavage in tau polymerization. We show that this fragment directly inhibits the in vitro polymerization of full-length and truncated tau, that it does so by interacting with one of the MTBRs, and that it likely assumes the configuration of an amphipathic helix in doing so.

† Supported by NIH Awards AG09465 and AG14453 to L.I.B. and a grant from the Alzheimer's Association to V.L.C.

* Corresponding author. Phone: (312) 503-8019, 0824. Fax: (312) 503-7912. E-mail: r-berry@northwestern.edu.

‡ Department of Cell and Molecular Biology.

§ Cognitive Neurology and Alzheimer's Disease Center.

|| Division of Endocrinology, Metabolism, and Molecular Medicine.

[1] Abbreviations: AD, Alzheimer's disease; i_s, intensity of scattered light; LLS, laser light scattering; MTBR, microtubule binding repeat; TFE, trifluoroethanol.

10.1021/bi027348m CCC: $25.00
Published on Web 06/17/2003

MATERIALS AND METHODS

Recombinant Proteins. The full-length tau used in this study was the recombinant htau 40, 441 residues in length, which corresponds to the longest tau isoform found in the central nervous system. Generation of the tau 1−421 truncation mutant is described in Gamblin et al. (unpublished). The tau 1−320 truncation mutant was the construct generated by Carmel et al. (*11*), and the tau 1−375 construct was described by Abraha et al. (*6*). All constructs were His-tagged at the amino terminus, expressed in *Escherichia coli*, and purified as previously described (*6*, *11*). The His-tag has no effect on arachidonic acid-induced tau polymerization (*12*).

Synthetic Peptides. The peptides used in this study were synthesized by Cell Essentials (Boston, MA) and supplied at 95% purity. Tau 422−441 (SPQLATLADEVSASLAKQGL) represents the C-terminal caspase cleavage fragment of tau. RND1 (SEGASLKLQVLTDPASAQAL) is a rearrangement of the same residues predicted to form an α-helix by the method of Chou and Fasman (*13*). RND2 (SDQLAPLAPEVSAGLAKQSL) differs from tau 422−441 by substitution of a proline for threonine at the sixth position and switching residues 2 for 9 and 14 for 19. This results in a peptide that is not predicted to form an α-helix.

Polymerization Reactions. Tau polymerization was induced by arachidonic acid as previously described (*14*). Briefly, the polymerization mixture contained tau protein (4 μM) in 10 mM HEPES, pH 7.4, with 100 mM NaCl and 5 mM dithiothreitol, to which was added 0−100 μM peptide. Arachidonic acid (Cayman Chemical, Ann Arbor, MI) was then added to 75 μM to initiate polymerization. Polymerization was monitored by right-angle laser light scattering (LLS) for 6 h at room temperature as described previously (*14*). The data were fit by nonlinear regression to one- or two-phase exponential association curves, using GraphPad Prism 3.0 software.

Unless otherwise noted, the LLS curves in this report represent combined data from three to five independent experiments. The rapid initial kinetics of polymerization and the fact that our apparatus is not automated made it impractical to monitor more than six reactions in one run. One of these was always htau 40 without peptide additions, and the others consisted of a tau construct with varying concentrations of peptide, including no peptide if the construct was not htau 40. When RND1 and RND2 were being tested, one reaction always consisted of truncated tau and the 422−441 peptide.

Quantitative Electron Microscopy. Polymerization reactions were allowed to proceed for 6 h, at which point samples were fixed in a final concentration of 2% glutaraldehyde for EM analysis. EM grids were prepared and negatively stained with 2% uranyl acetate to enable quantification of the tau filaments as previously described (*14*). Samples were examined using the JEOL JEM-1220 electron microscope at 60 kV and 20 000× magnification, and a series of five random photographs was taken from each grid for analysis using a Kodak 1.6I Megaplus digital camera and AMT camera driver software. Images were calibrated using 200 nm diameter beads on a grating replica (Electron Microscopy Sciences). Images were processed in Adobe Photoshop 5.0, and quantification was done using Optimas 6.5 (Media Cybernetics) software, all as described previously (*14*). Briefly, brightness and contrast were altered for optimum visualization, and the image was smoothed and thresholded. The average mass of filaments within a field (± sem) was calculated by multiplying the field's average filament length, as determined by Optimas, by the average filament number.

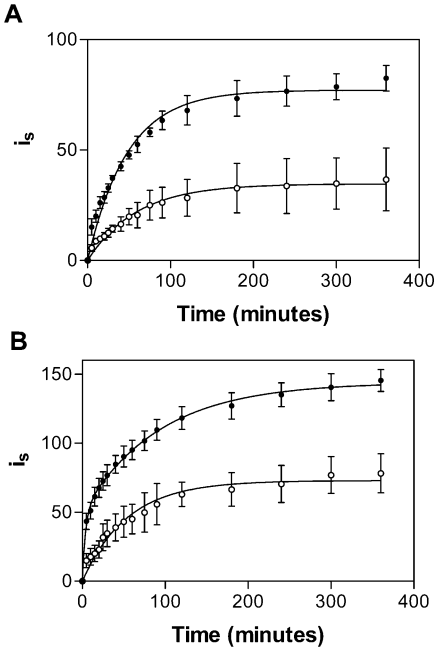

FIGURE 1: Inhibition of polymerization of full-length and truncated tau by the C-terminal peptide. (A) Time course of the polymerization of 4 μM htau 40 in the absence (solid circles) and presence (open circles) of 100 μM tau 422−441 as measured by LLS. The intensity of scattered light (i_s) on the ordinate reflects the mass of polymerized material (*13*). Except where noted, in this and all subsequent figures, data is plotted as the mean ± sem of at least three measurements. (B) Time course of the polymerization of 4 μM tau 1−421 in the absence (solid circles) and presence (open circles) of 100 μM 422−441 peptide as measured by LLS.

Circular Dichroism. The circular dichroism (CD) spectra of tau 422−441, RND1, and RND2 were obtained at 20 °C with a Jasco 715 spectrometer using a 2 mm path length quartz cuvette. For these measurements, the peptides were diluted to a concentration of 0.1 mg/mL (50 μM) in 10 mM potassium phosphate buffer, pH 7.6, or in this same buffer containing 36% trifluoroethanol (TFE, Fluka). The curves shown in this report represent the average of four runs. The CD data is expressed as [Θ], the molar ellipticity, in units of deg cm^2 $dmol^{-1}$.

RESULTS

C-Terminal Caspase Cleavage Fragment Inhibits Polymerization of Full-Length and Truncated Tau. We first asked if tau 422−441 would inhibit the polymerization of the full-length htau 40. As shown in Figure 1A, this peptide inhibited the extent of polymerization of intact tau by approximately 50% at the highest concentrations tested. It also produced a lengthening of the half-time of polymerization from 33 to 41 min, but this was not statistically significant.

We next investigated the effect of tau 422−441 on polymerization of recombinant tau truncated at the caspase cleavage site, Asp 421 (this N-terminal caspase cleavage product encoding amino acids 1−421 is referred to as truncated tau throughout the text). The polymerization of the

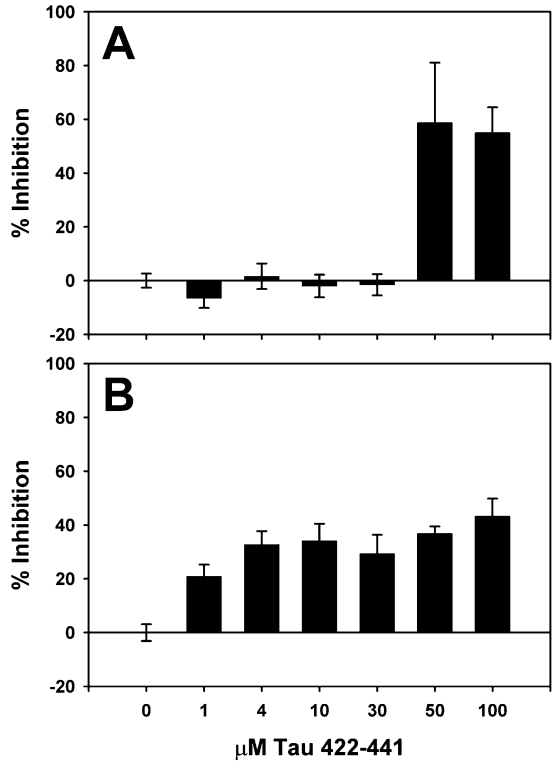

FIGURE 2: Dose−response curves for inhibition of polymerization of full-length and truncated tau by tau 422−441. (A) Concentration dependence of the inhibition of polymerization of htau 40 by the peptide. (B) Concentration dependence of the inhibition of polymerization of tau 1−421 by the peptide. In both cases, 4 μM tau was used.

truncated protein differs from that of its full-length counterpart in both extent and kinetics. As we report elsewhere (Gamblin et al., unpublished), truncated tau exhibits a greater extent of polymerization (67% greater in these experiments—compare Figure 1B to 1A). In addition, with a half-time of 3 min, truncated tau polymerizes approximately 10 times faster than full-length tau.

As was the case for full-length tau, the C-terminal caspase cleavage fragment also inhibits polymerization of truncated tau, again by about 50%, resulting in nearly the same amount of polymerization as full-length tau in the absence of the peptide (Figure 1B). Tau 422−441 slows the rate of polymerization of truncated tau dramatically (half-time of 21 min at 100 μM peptide versus 3 min in its absence).

The dose−response curve of inhibition of polymerization of full-length tau exhibits a sharp transition between 30 and 50 μM peptide (Figure 2A). Thus, to be effective, the peptide must be present at about 10 times the concentration of the intact protein. The C-terminal peptide is significantly more potent in inhibiting polymerization of the truncated protein, however, achieving 25% inhibition at an equimolar concentration (4 μM), and increasing to nearly 50% at 100 μM (Figure 2B).

We have shown previously that, in LLS, i_s is an accurate measure of the mass of polymerized full-length tau (*14*). However, we have also shown that N-terminally modified tau constructs can form aggregates that scatter less efficiently than normal tau (*15*). Therefore, to confirm the results obtained by LLS, the filaments formed by full-length htau 40 in the presence and absence of 100 μM tau 422−441 peptide were analyzed by quantitative negative stain EM

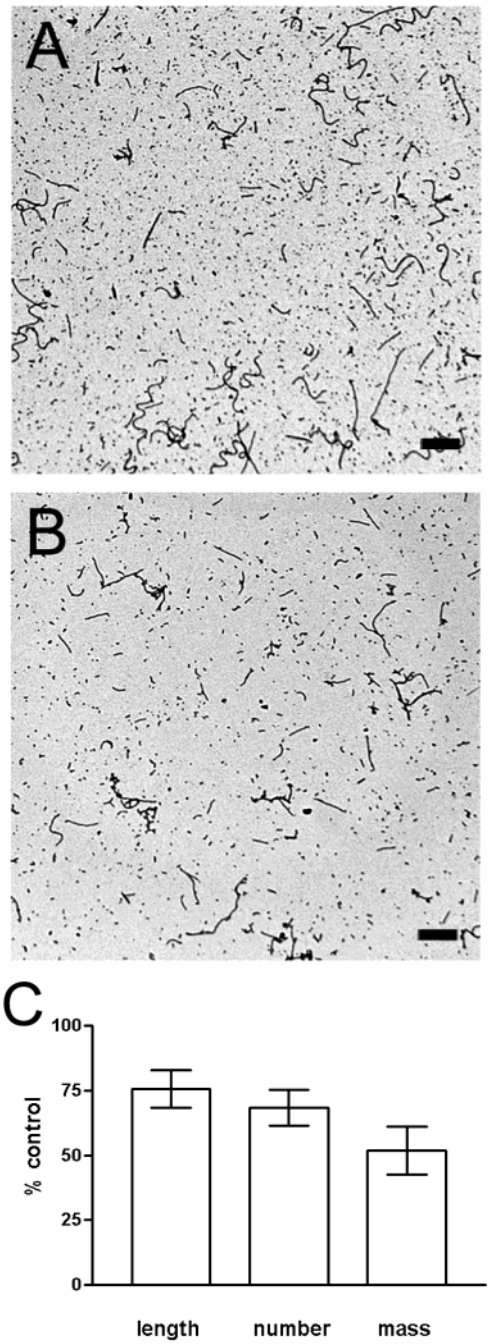

FIGURE 3: Representative digital negative stain electron micrographs (20 000×) of filaments generated from full-length htau 40 in the absence (A) and presence (B) of 100 μM 422−441 peptide. The size bar represents 500 nm. The graph (C) shows the result of quantitative electron microscopy measurements from three separate experiments. The average filament length, number, and mass per field formed in the presence of the peptide are expressed as a percentage of that formed in the absence of the peptide. Error bars represent the standard error of the mean.

(Figure 3). In three separate experiments, addition of this peptide reduced the average number of filaments per field to 68% (±7% sem) that of the control, and the average length of the filaments was 76% (±7% sem) that of the control. This translated into an approximate 50% decrease in the average mass of filaments per field (−48 ± 9% sem), which is in close agreement with the LLS results (Figure 2C).

Inhibition of Tau Polymerization Requires Part of the Microtubule Binding Region. To identify the region of the

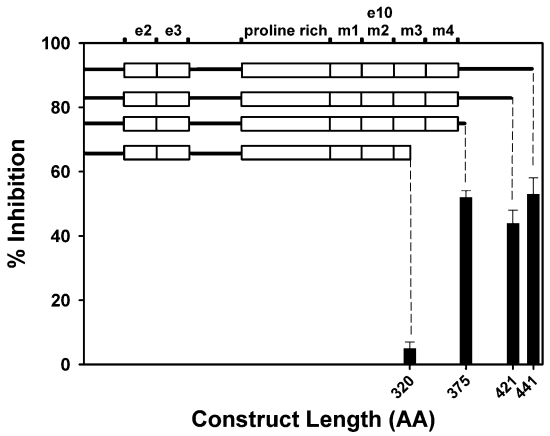

FIGURE 4: Residues 321−375 are required for the inhibitory effect of the 422−441 peptide. The upper figures are schematic representations of the tau constructs tested: from top to bottom, htau 40 (1−441), 1−421, 1−375, and 1−320. e2, e3, and e10 are tau's variably present exons, m1−m4 are the MTBRs. Bars give the mean ± sem of the percent inhibition of polymerization of each construct by the 422−441 peptide.

tau molecule that interacts with the C-terminus to inhibit polymerization, we employed a series of truncation mutants. We have previously demonstrated that in the absence of peptide additions, each of the truncation mutants used in the present study polymerizes to approximately the same extent (*6*). To assess inhibition, we compared the extent of polymerization at the end of 6 h in the presence or absence of the tau 422−441 peptide. The results, presented in Figure 4, are unambiguous: the C-terminal peptide inhibits polymerization by about 50% in tau mutants that contain residues C-terminal to position 375, but inhibition is lost upon removal of residues 321−375. This truncation removes about half of the third MTBR and all of the fourth. Although the tau 1−320 construct cannot be inhibited by the tau 422−441 peptide, in the absence of peptide it assembles as efficiently as the other constructs that are truncated nearer the C-terminus and to a greater extent than htau 40 (*6*).

Helical Conformation of the C-Terminus Is Important for Inhibition of Tau Polymerization. Although there is evidence that the tau molecule possesses minimal secondary structure in solution (*2*, *3*), there is also evidence that the C-terminal region is capable of adopting an α-helical conformation (*16*, *17*). Moreover, a helical wheel projection predicts that such a conformation would result in an amphipathic helix, with opposite polar and nonpolar faces (Figure 5A). By segregating residues with similar polarity, amphipathic helices are important determinants of tertiary structure in many proteins (*18*).

To assess the importance of secondary structure in the function of the C-terminal peptide, we investigated two additional synthetic peptides having the same or nearly the same amino acid compositions but widely different predicted secondary structures. The first, RND1, had precisely the same amino acid composition as tau 422−441, but in a different order, yet was also predicted to assume an amphipathic helical conformation (Figure 5B). The other, RND2, had the same amino acid composition, with the exception of a Thr to Pro substitution, and a sequence predicted not to be conducive to helix formation (see Materials and Methods).

We performed circular dichroism measurements to confirm the secondary structural predictions. We assessed the degree of helical conformation in aqueous polymerization buffer and in buffer to which trifluoroethanol (TFE) had been added to a concentration of 36%. The former condition reproduces the environment of the peptides in solution, while the latter is frequently employed to mimic the hydrophobic microenvironment of a peptide domain within a folded protein structure (*19*). As shown in Figure 5A, and as predicted from previous reports (*16*, *17*), tau 422−441 exhibits little secondary structure in aqueous buffer but in the hydrophobic environment afforded by 36% TFE assumes substantial helical structure, as assessed by the development of minima at 208 and 223 nm. The scrambled peptide, RND1, had an equal to or greater propensity for helix formation (Figure 5B), and the RND2 peptide showed little tendency to assume an ordered conformation (Figure 5C).

The helix-forming peptide, RND1, inhibited polymerization of tau 1−421 by about 25%, or by approximately half the extent as tau 422−441 (Figure 6). On the other hand, the nonhelical peptide, RND2, had little effect on tau polymerization, particularly in the initial more rapid phase of assembly (Figure 6); the plateau level of polymerization was not significantly affected ($P = 0.28$).

DISCUSSION

We have previously demonstrated that various truncations of the tau molecule C-terminal to the MTBR region promote polymerization (*6*). Truncation at Asp 421 is of particular interest because it is the cleavage site for caspases, a conserved family of proteases that induce apoptosis by specifically proteolyzing substrates at aspartate residues (reviewed in ref *20*). Recent evidence has been adduced linking caspase cleavage of tau to Alzheimer's disease, the most prevalent of the dementing neurodegenerative disorders (Gamblin et al., unpublished). The present study complements the work with truncation mutants by showing that, when added back to either the full-length or the cleaved parent molecule, a synthetic peptide identical to the caspase-generated fragment inhibits tau polymerization, thus supporting the contention that caspase cleavage promotes assembly by removing the inhibitory effects of the C-terminus on polymerization. In addition, these experiments speak to the mechanism of tau polymerization and raise additional issues concerning this process. These are discussed below.

Tau 422−441 Likely Interacts with the MTBR. The results presented in Figure 4 indicate that the C-terminal caspase cleavage fragment retains its inhibitory activity with C-terminally truncated tau constructs as short as tau 1−375 but loses this activity when the 321−375 region is deleted. These observations suggest that the C-terminal peptide inhibits polymerization by binding to some portion of this region. It is conceivable that removal of the 321−375 region alters the structure of other regions of the tau molecule to disrupt binding of the 422−441 peptide; however, the fact that tau 1−320 polymerizes equally as well as the more distal truncations (*6*) argues strongly against this hypothesis.

The delineation of the region of interaction is an important finding in two respects. First, the fact that the untethered peptide is effective indicates that inhibition is likely a direct consequence of binding and is not secondary to a torsion of the intervening region induced by that binding. We note in

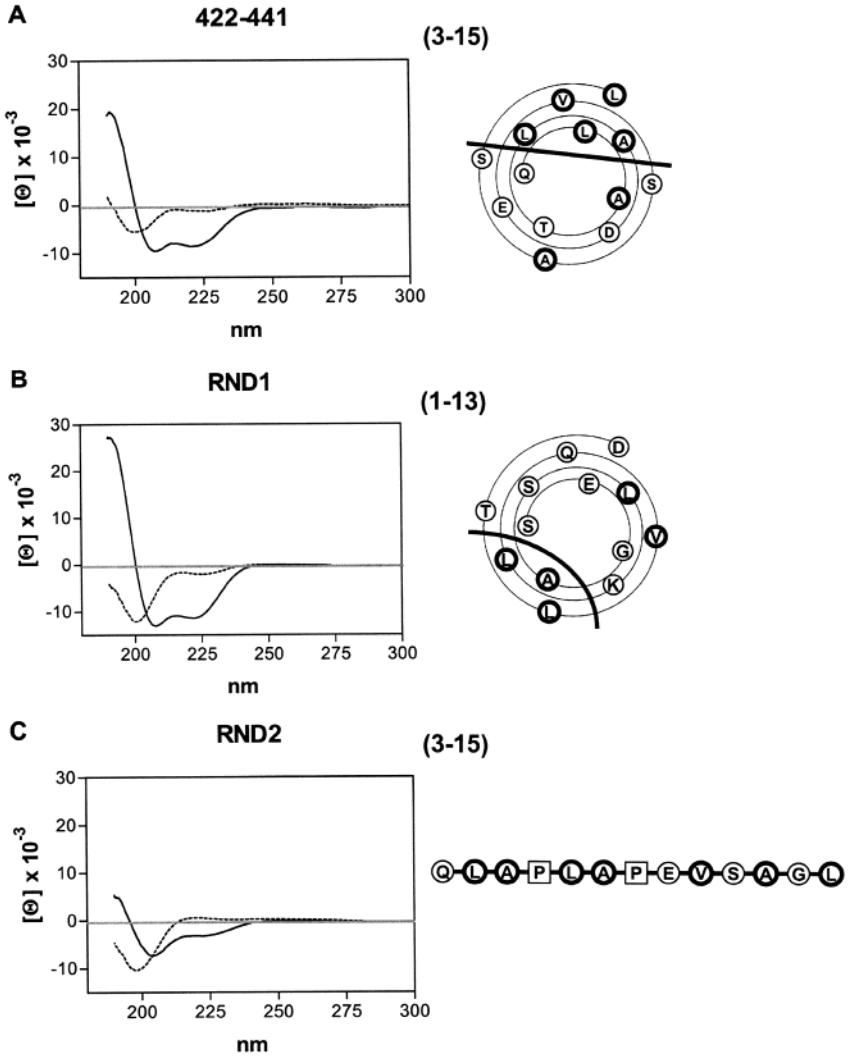

FIGURE 5: Circular dichroism measurements and predicted structures of the three peptides used in this study. On the left, molar ellipticity, [Θ], is plotted against wavelength for (A) tau 422−441, (B) RND1, and (C) RND2 in the absence (dotted lines) and presence of 36% TFE (dark solid lines). On the right: (A) projection in α-helical geometry of residues 3−15 in the tau 422−441 peptide. (B) Projection in α-helical geometry of residues 1−13 in RND1. In both cases, the heavier circles denote nonpolar residues, and the nonpolar face of each helix is delimited by a dotted line. In these projections, the innermost residue is the most N-terminal. (C) The sequence of residues 3−15 of RND2, which is predicted to have no predilection for secondary structure, largely because of the presence of prolines at positions 6 and 9.

this context that in similar experiments a peptide consisting of tau residues 1−15 had no effect on tau polymerization, although a deletion of this region did (*15*). This suggests that, in contrast to the C-terminus, the domain represented by the N-terminal peptide must be tethered to have an effect.

Identification of the likely region of interaction is also important because of its location in the MTBR. As noted in the introductory paragraphs, the MTBR has been implicated as being crucial to tau aggregation in both in vitro and in situ studies. The region of putative peptide binding is immediately adjacent to residues 314−320, which have been shown to be essential for the fatty acid induction of tau polymerization (*6*). Moreover, an adjoining region, residues 306−311, has been implicated in the induction of tau polymerization by polyanions (*4*). It seems reasonable to propose that binding of the C-terminus disturbs interactions in these regions that normally encourage polymerization. A likely candidate for such an interaction is an association between the MTBR and tau's amino terminus (*15*), which leads to the formation of the Alz 50 epitope (*11*, *21*). This epitope may arise early in the course of neurofibrillary tangle formation, as it appears early in AD (*5*).

The difference in the dose−response curves for the tau 422−441 peptide with full-length and truncated tau is of interest, as presumably it is due to competition between the peptide and the cognate region of the intact protein for the MTBR site. The EC_{50} of the peptide for tau 1−421 is ≤4 μM, or roughly equivalent to the concentration of tau protein. However, the peptide's EC_{50} is about 10-fold greater for the intact protein. Thus, the presence of the carboxy-terminus interferes with the peptide's ability to interact with its binding site on the protein. This may be due to steric hindrance by the C-terminus, which, although not bound to the site, by virtue of being tethered to it, would necessarily be in the vicinity.

Inhibition May Require that Tau 422−441 Assume an α-Helical Configuration. As anticipated from previous reports (*16*, *17*), the C-terminal fragment displays a tendency to assume a helical structure in a mildly hydrophobic environment (Figure 5A). Although counter-examples exist

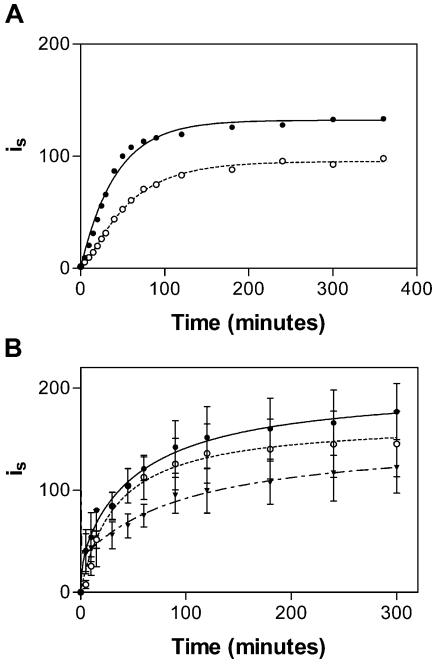

FIGURE 6: Influence of the peptides RND1 and RND2 on the polymerization of tau 1−421. (A) Time course of the polymerization of 4 μM tau 1−421 in the absence (solid circles) and presence (open circles) of 50 μM RND1 peptide as measured by LLS. The values are means of two replicates. (B) Time course of the polymerization of 4 μM tau 1−421 in the absence (solid circles) and presence of 100 μM RND2 peptide (open circles) or tau 422−441 (solid triangles).

(*19*), this behavior is frequently taken to mean that the peptide in question forms an α-helix in the intact protein (*19*). To test the role of this conformation in the inhibition of tau polymerization, we assessed the effect of two synthetic peptides with similar amino acid compositions, one of which (RND1) displayed a propensity for helix formation in TFE, the other of which (RND2) did not. As predicted, RND1 was partially effective in inhibiting tau polymerization, while the effect of RND2 was minimal. The C-terminus and the peptide RND1 form α-helical structures, both of which are predicted to be amphipathic (Figure 5). Moreover, they both inhibit polymerization, whereas a similar peptide with little tendency to form an α-helical structure does not inhibit assembly. Thus, it is likely that an amphipathic helical structure is important for the inhibition. However, the fact that RND1 activity was diminished in comparison to that of the tau 422−441 peptide suggests that the actual sequence of residues in tau's C-terminus is also important for this interaction.

Model for the Inhibition of Polymerization by Tau's C-Terminus. The foregoing suggests that the C-terminus inhibits tau polymerization by interacting as an amphipathic helix with a stretch of residues between Cys 322 and Lys 375. Since amphipathic helices frequently interact with other amphipathic helices, it is possible that some portion of this stretch of residues also forms an amphipathic helix. In fact, it has been reported recently that residues 315−325 in the third MTBR form just such a helix and that this helix is important to the polymerization process (*22*). It is unlikely that the C-terminal peptide interacts directly with this particular region of the third MTBR since it does not inhibit the polymerization of tau 1−320. It is also unlikely that the truncation at residue 321 disrupts the structure of this region since tau 1−320 polymerizes quite readily (*6*). However, sequence analysis of the three other MTBRs suggests that they too should be capable of adopting α-helical structures with similar hydrophobic patches. In particular, residues 346−357 in the fourth MTBR share this property with the analogous stretch in MTBR 3. We propose, therefore, that the C-terminus binds to an amphipathic α-helix in MTBR 4 and inhibits other interactions of this helix that would be favorable for polymerization.

Just what these interactions might be remains a matter of speculation at this point, but one attractive possibility is that an amphipathic helix in MTBR 4 and a similar helix in one of the other MTBRs bind along their hydrophobic faces and that this induces in the tau molecule the Alz 50 conformation that favors polymerization. A mechanism of this type would be consistent with the recent demonstration of a high α-helical content of the tau in paired helical filaments from AD brain (*23*). Thus, the C-terminus may inhibit polymerization via a domain swap mechanism (*24*), substituting for the MTBR helix that binds to MTBR 4.

In summary, our data indicate that the seemingly structureless nature of the tau molecule could be misleading. The same flexibility that is responsible for tau's random coil appearance in aqueous solution permits ready conformational transformations, perhaps controlling the structure and display of the MTBRs through alternative interactions with the C- and N-termini. Conceivably, these molecular rearrangements could determine tau's ability to bind to the microtubule lattice, to dissociate from the microtubule and form homopolymers, or to disengage from the microtubule and remain harmlessly unbound in the cytosol.

ACKNOWLEDGMENT

We wish to thank Dr. J. Kuret of Ohio State University for use of the tau 1-320 construct and Dr. B. Shoichet of Northwestern for materials, advice, and assistance with the circular dichroism measurements.

REFERENCES

1. Lee, V. M., Goedert, M., and Trojanowski, J. Q. (2001) *Annu. Rev. Neurosci. 24*, 1121−59.
2. Cleveland, D. W., Hwo, S. Y., and Kirschner, M. W. (1977) *J. Mol. Biol. 116*, 227−47.
3. Schweers, O., Schonbrunn-Hanebeck, E., Marx, A., and Mandelkow, E. (1994) *J. Biol. Chem. 269*, 24290−7.
4. von Bergen, M., Friedhoff, P., Biernat, J., Heberle, J., and Mandelkow, E. (2000) *Proc. Natl. Acad. Sci. U.S.A. 97*, 5129−34.
5. Garcia-Sierra, F., Ghoshal, N., Berry, R. W., Quinn, B., and Binder, L. I. (2003) *J. Alzheimer's Dis. 5*, 65−77.
6. Abraha, A., Ghoshal, N., Gamblin, T. C., Cryns, V., Berry, R. W., Kuret, J., and Binder, L. I. (2000) *J. Cell Sci. 113*, 3737−45.
7. Fasulo, L., Ugolini, G., Visintin, M., Bradbury, A., Brancolini, C., Verzillo, V., Novak, M., and Cattaneo, A. (2000) *J. Neurochem. 75*, 624−33.
8. Chung, C. W., Song, Y. H., Kim, I. K., Yoon, W. J., Ryu, B. R., Jo, D. G., Woo, H. N., Kwon, Y. K., Kim, H. H., Gwag, B. J., Mook-Jung, I. H., and Jung, Y. K. (2001) *Neurobiol. Dis. 8*, 162−72.
9. Jordan, J., Galindo, M. F., and Miller, R. J. (1997) *J. Neurochem. 68*, 1612−21.
10. Troy, C. M., Rabacchi, S. A., Friedman, W. J., Frappier, T. F., Brown, K., and Shelanski, M. L. (2000) *J. Neurosci. 20*, 1386−92.
11. Carmel, G., Mager, E. M., Binder, L. I., and Kuret, J. (1996) *J. Biol. Chem. 271*, 32789−95.

12. King, M. E., Gamblin, T. C., Kuret, J., and Binder, L. I. (2000) *J. Neurochem. 74*, 1749−57.
13. Chou, P. Y., and Fasman, G. D. (1974) *Biochemistry 13*, 211−22.
14. Gamblin, T. C., King, M. E., Dawson, H., Vitek, M. P., Kuret, J., Berry, R. W., and Binder, L. I. (2000) *Biochemistry 39*, 6136−44.
15. Gamblin, T. C., Berry, R. W., and Binder, L. I. (2003) *Biochemistry 42*, 2252−7.
16. Yanagawa, H., Chung, S. H., Ogawa, Y., Sato, K., Shibata-Seki, T., Masai, J., and Ishiguro, K. (1998) *Biochemistry 37*, 1979−88.
17. Esposito, G., Viglino, P., Novak, M., and Cattaneo, A. (2000) *J. Pept. Sci. 6*, 550−9.
18. Brèandâen, C.-I., and Tooze, J. (1999) *Introduction to protein structure*, 2nd ed., Garland Pub., New York.
19. Waterhous, D. V., and Johnson, W. C., Jr. (1994) *Biochemistry 33*, 2121−8.
20. Cryns, V., and Yuan, J. (1998) *Genes Dev. 12*, 1551−70.
21. Jicha, G. A., Berenfeld, B., and Davies, P. (1999) *J. Neurosci. Res. 55*, 713−23.
22. Minoura, K., Tomoo, K., Ishida, T., Hasegawa, H., Sasaki, M., and Taniguchi, T. (2002) *Biochem. Biophys. Res. Commun. 294*, 210−4.
23. Sadqi, M., Hernandez, F., Pan, U., Perez, M., Schaeberle, M. D., Avila, J., and Munoz, V. (2002) *Biochemistry 41*, 7150−5.
24. Liu, Y., Gotte, G., Libonati, M., and Eisenberg, D. (2001) *Nat. Struct. Biol. 8*, 211−4.

BI027348M